Catalysis Letters Vol. 113, Nos. 1–2, January 2007 (© 2007)
DOI: 10.1007/s10562-006-9004-6

Hydrothermal synthesis of flaky crystallized $La_2Ti_2O_7$ for producing hydrogen from photocatalytic water splitting

Haibo Song[a], Tianyou Peng[a,c,*], Ping Cai[a], Huabing Yi[a], and Chunhua Yan[b]

[a]*Department of Chemistry, Wuhan University, Wuhan, 430072 China*
[b]*State Key Laboratory of Rare Earth Materials Chemistry and Applications, Peking University, Beijing, 100871 China*
[c]*Hubei Key Laboratory for Catalysis and Material Science, South-Central University for Nationalities, Wuhan, 430074 China*

Received 29 September 2006; accepted 15 November 2006

Flaky monoclinic $La_2Ti_2O_7$ was prepared *via* a hydrothermal method based on the reaction of $Ti(SO_4)_2$ and $La(NO_3)_3$. Relative to the solid-state reaction sample, the flaky $La_2Ti_2O_7$ showed higher surface areas, much smaller crystal size and more efficient light absorption. All these factors led to the higher photoactivity to produce H_2 from water splitting under UV irradiation.

KEY WORDS: $La_2Ti_2O_7$; hydrothermal synthesis; photocatalytic activity; water splitting.

1. Introduction

Monoclinic compounds $La_2Ti_2O_7$ with space group $P2_1$ has been the subject of considerable interests due to its properties as photocatalyst for producing hydrogen from water photosplitting and photodegradation of organic pollutants [1–5]. $La_2Ti_2O_7$ was initially prepared by a conventional solid-state reaction (SSR) method [6, 7], in which appropriate amounts of precursor oxides or carbonates are ground together and then calcined at a high temperature (1100–1400 °C) for long periods to allow interdiffusion of cations. This method produces materials with low surface areas, nonuniform particle sizes and low phase purity, and in consequence, a low photoactivity for the water splitting.

Attempts to synthesize $La_2Ti_2O_7$ below 900 °C have been carried out through several solution techniques to get active photocatalysts with high surface areas, such as coprecipitation [4], metal organic decomposition [5], sol–gel [8] and polymerized complex method [3, 9, 10]. For example, $La_2Ti_2O_7$ have been prepared by the polymerized complex method, which was reported to have a high surface area due to the relative low heat treatment temperature, and also to exhibit much higher activity than the photocatalyst prepared by the SSR method for the photocatalytic water decomposition under ultraviolet (UV) irradiation [11, 12]. M-doped $La_2Ti_2O_7$ (M = Cr, Fe) as photocatalyst has also been fabricated for the water splitting under visible light irradiation [1]. A highly donor-doped (110) layered $La_2Ti_2O_7$ has also been found to be an efficient photocatalyst for the degradation of organic pollutants, which is comparable to TiO_2 (P25) [2]. Moreover, this photocatalysts loaded with nickel show high quantum yields for the water photosplitting [3, 13–15]. However, the surface areas of these materials are still very small due to the high-temperature treatment needed to obtain crystalline phases. Therefore, it still remains essentially important to seek for more effective method for the preparation of $La_2Ti_2O_7$ under mild synthetic conditions. To the best of our knowledge, there are only a few studies focused on the hydrothermal synthesis of $La_2Ti_2O_7$ [16, 17]. Herein, a flaky monoclinic $La_2Ti_2O_7$ was fabricated from the reaction of $La(NO_3)_3$ and $Ti(SO_4)_2$ via a hydrothermal reaction by using cetyltrimethylammonium bromide (CTAB) as surfactant and NaOH as mineralizer. The microstructures, optical property, and photoactivities of $La_2Ti_2O_7$ are studied in detail.

2. Experimental section

In a typical procedure, a $Ti(SO_4)_2$ solution was added into CTAB solution under stirring, and then $La(NO_3)_3$ solution was slowly added into above mixture. The molar ratio of $La(NO_3)_3$:$Ti(SO_4)_2$:CTAB is 1:1:0.2, the pH value of the mixture was then adjusted by a supersaturated NaOH solution. After stirring for 30 min, the resulting mixture was aged at room temperature for 12 h and then transferred into a Teflon-lined autoclave, which was maintained at 150–240 °C for 24 h. The product was collected by centrifugation, washed with distilled water and ethanol in sequence, and then dried at 80 °C overnight. Ion-exchange treatment was performed to remove

*To whom correspondence should be addressed.
E-mail: typeng@ whu.edu.cn

CTAB by mixing the as-synthesized powders with a water–ethanol solution of NaCl under stirring at 40 °C for 10 h. $La_2Ti_2O_7$ was also prepared from mixture of La_2O_3 (99.99%) and TiO_2 (rutile) at 1150 °C according to SSR method [7].

The obtained samples were characterized by X-ray powder diffraction (XRD) analyses using XRD-6000 diffractometer, transmission electron microscopy (TEM) on LaB6 JEM-2010 (HT)-FEF electron microscope and field emission scanning electron microscopy (FESEM) on FEG SEM Sirion electron microscope. The nitrogen adsorption and desorption isotherms at 77 K were measured on a Micrometrics ASAP 2010 system after samples were degassed at 120 °C. UV–Vis diffuse reflectance spectra (DRS) were performed with a Cary 5000 UV–Vis–NIR spectrophotometer equipped with an integrating sphere.

Photocatalytic reaction was performed at room temperature in an outer-irradiation-type Pyrex reactor (320 mL). A 500 W high-pressure mercury lamp was applied as light source, which is positioned inside a cylindrical Pyrex vessel surrounded by a circulating water jacket (Pyrex) to cool the lamp. A cylindrical Pyrex glass vessel was used as photoreactor, which were located at 15 cm's distance to the Hg lamp. The catalyst (0.0500 g) was suspended in distilled water (200 mL) by magnetic stirring. The rates of H_2 evolution were determined by gas chromatography (TCD, molecular sieve 5 Å columns and Ar carrier).

3. Results and discussion

The XRD patterns for the products showed that maintaining the hydrothermal system at 210–240 °C for 20–24 h (pH 12.5) is the most suitable synthetic conditions for $La_2Ti_2O_7$. The XRD patterns for the obtained $La_2Ti_2O_7$ powders are shown in figure 1. The sample derived from 180 °C was only composed of the diffraction peaks attributed to La_2O_3 and $La(OH)_3$. There is no any significant reflection peak attributed to $La_2Ti_2O_7$ and TiO_2. While all reflection peaks for the SSR sample completely accord with those of monoclinic $La_2Ti_2O_7$ reported in JCPDS 28-0517. The product prepared from the hydrothermal treatment at 210 °C for 24 h show good agreement with those of monoclinic $La_2Ti_2O_7$, and the crystallinity of the product was enhanced upon increasing the hydrothermal temperature from 210 to 240 °C, all XRD reflections for the sample derived from 240 °C exhibited a single phase of monoclinic $La_2Ti_2O_7$. This result indicates that the crystallization of $La_2Ti_2O_7$ is completed between 210 °C and 240 °C. The crystal sizes, calculated by Scherrer's equation, are ca. 15.9 nm (210 °C), 17.5 nm (240 °C), and 52.6 nm (SSR), respectively. Thus, the crystallized $La_2Ti_2O_7$ with much small crystal size is formed by the hydrothermal method. The calculated cell parameters, based on the XRD data (Table 1), are similar with those of SSR product and the JCPDS 28-0517, indicating that the $La_2Ti_2O_7$ with monoclinic structure can be formed at significantly lower temperature and shorter reaction time comparing with the SSR sample and the previous publications [2–7]. Relative to the SSR sample, however, the XRD patterns for the products derived from hydrothermal processes show weaker and broader diffraction peaks, and the intensities of those main diffraction peaks assigned to monoclinic $La_2Ti_2O_7$ also exist obvious differences between the two kinds of samples as observed from figure 1. Moreover, there are two undistinguishable broad diffraction peaks between $2\theta = 27$–$29°$ and 31–34° for the hydrothermal samples, whereas the SSR sample shows distinguishable sharp diffraction peaks. Namely, those experimental facts indicate that the hydrothermal samples have much smaller crystal sizes and the lower crystal perfection than that of SSR sample.

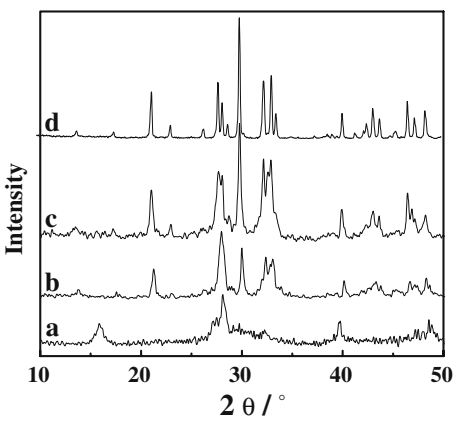

Figure 1. XRD patterns of $La_2Ti_2O_7$ obtained from hydrothermal reaction. (a) 180 °C, (b) 210 °C, (c) 240 °C, and (d) derived from SSR method.

Figure 2 shows the FESEM photographs for $La_2Ti_2O_7$ prepared by the hydrothermal and SSR method. The SSR product only consists of well-rounded particles with particle sizes in the range of 0.4–2.5 μm (figure 2c). These particles are agglomerates of crystallites with 52.6 nm in average sizes as measured by XRD analyses. Whereas, samples derived from hydrothermal processes consist of flakes in irregular shapes with the length and width in sub-micrometer scale. More detail morphologies of the flakes can be seen from the HRTEM images (figure 3). Figure 3a shows that the $La_2Ti_2O_7$ obtained at 210 °C consist mainly of nearly homogenous and laminar grains. Those laminar grains are present in irregular shapes with some concomitants of rectangular edges. The observed very faint contrasts indicate the very thin in thickness of the flaky grains. It is interesting to note the periodical fringes in HRTEM image of one flake (figure 3b), indicating that the single crystal of the layered $La_2Ti_2O_7$. Figure 3c shows a magnified lateral image of a thin flake, from which the

Table 1
The crystallite sizes, lattice parameters, BET surface areas and photocatalytic activity of $La_2Ti_2O_7$

Sample	a (Å)	b (Å)	c (Å)	Crystal sizes (nm)	S_{BET} ($m^2\ g^{-1}$)	Activity (μmol H_2/h g)
treated at 210 °C	13.084	5.536	7.829	15.9	82	50.44
treated at 240 °C	13.097	5.537	7.834	17.5	54	72.46
SSR at 1150 °C	13.010	5.544	7.810	52.6	1.1	0
JCPDS 28-0517	13.01	5.545	7.817	–	–	–

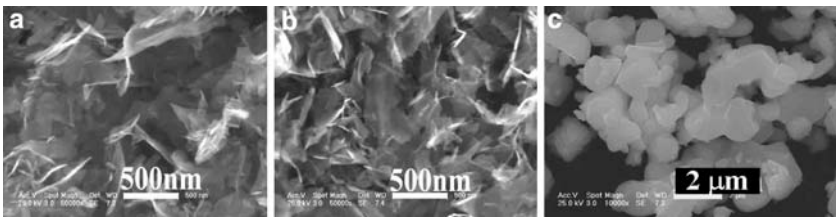

Figure 2. FESEM images of products derived from hydrothermal and SSR method. (a) hydrothermal treatment at 210 °C, (b) 240 °C, and (c) SSR method.

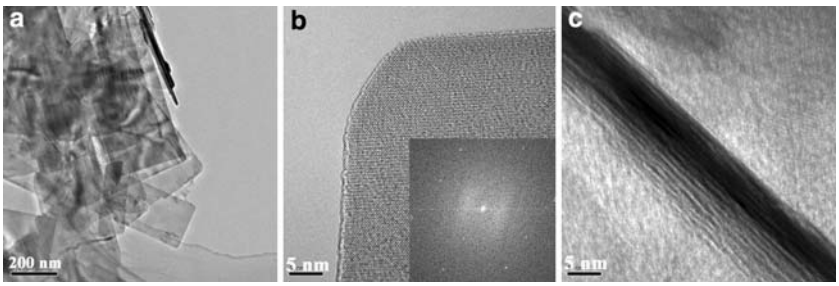

Figure 3. HRTEM photographs of products derived from hydrothermal reaction at 210 °C.

multilayer structure can be seen more clearly. In this case, the black stripes (ca. 1.0 nm thickness) correspond to slab thickness (1.054 nm) of the monoclinic $La_2Ti_2O_7$ [3], and the white stripes (ca. 0.25 nm thickness) closed to the inside of the flake correspond to the interlayer space (0.247 nm) of $La_2Ti_2O_7$ [3], indicating that the thin planar morphology of the sample has a full-grown $La_2Ti_2O_7$ crystallite, which is consistent with the observation of XRD. The selected area electron diffraction pattern (SAED) inserted in figure 3b also displays a symmetric array of sharp spots, indicating these laminar grains are single crystal. However, the very thin flaky morphologies and the smaller crystallite size of the hydrothermal samples might affect the crystal perfection of $La_2Ti_2O_7$, because the periodical crystal boundaries has been destroyed at least in the vertical directions of the thin flaky planes, which might result in a large amount of "broken" surfaces or dangling bonds and defect centers intrinsically existing in the hydrothermal samples [18]. It is also the inherent reason for the main diffraction peaks intensities of the hydrothermal samples are obvious different from that of SSR sample as observed from figure 1. Therefore, it can be concluded that the hydrothermal samples have much lower crystal perfection than that of SSR sample despite of the full-grown $La_2Ti_2O_7$ crystallite in the planar directions of the thin flakes.

Figure 4 depicts the EDAX pattern of the sample derived from 210 °C, there are two kinds of peaks in the EDAX pattern correspond to La and Ti, which shows the atom ratio of La and Ti is 1:1. Moreover, the EDXA result in figure 4 also shows that there exists very small

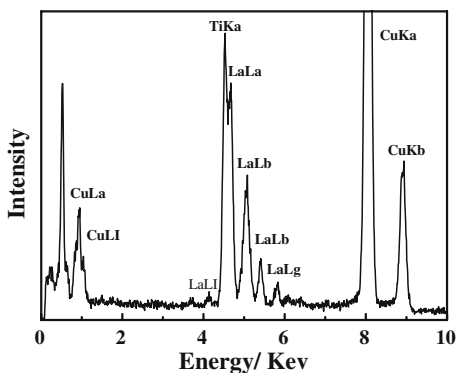

Figure 4. EDAX spectrum of product derived from hydrothermal reaction at 210 °C.

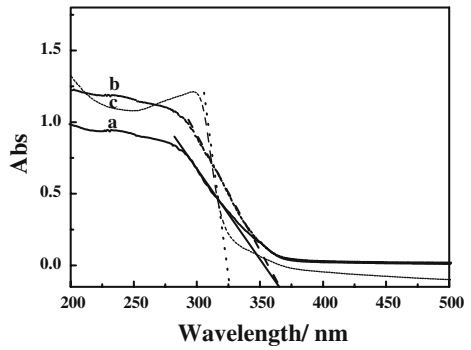

Figure 5. DRS spectra of products derived from hydrothermal and SSR method. (a) hydrothermal treatment at 210 °C, (b) at 240 °C, and (c) SSR method.

amount of C atom, which may be attributed to the remaining pyrolyzing products of the surfactant (CTAB). Whereas there is no any signal assigned to the IR peaks for the carbonate ion at 1738, 1096 and 798 cm^{-1} in the IR spectra (not shown) [18]. Furthermore, the XRD patterns for the hydrothermal samples (figure 1) also show no any diffraction peak assigned to Ti–C, indicating that the amount of C atom in $La_2Ti_2O_7$ is very small, and consequently its IR and XRD peaks are considered to be very weak [18].

Figure 5 shows the UV–Vis diffuse reflectance spectra (DRS) for the samples derived from the hydrothermal and SSR method. The wavelength at the absorption edge (λ_{ab}) was determined as the intercept on the wavelength axis for a tangent line as drawn in figure 5. The main λ_{ab} of both the hydrothermal samples are estimated to be about 365 nm (3.40 eV). Whereas, the main λ_{ab} of the SSR sample is about 325 nm (3.82 eV), which is consistent with the literature value [1, 3]. The band gap absorption of the hydrothermal samples has some red-shift, which might make them show better efficiency for the water photosplitting than that of SSR sample. Moreover, the DRS spectra for the hydrothermal samples show also tails with higher light absorption at long wavelength side compared with the SSR sample. Obviously, this visible absorbance cannot be attributed to a band-to-band transition of $La_2Ti_2O_7$ [7]. Wang and co-workers had reported a similar phenomenon [19], they found that the band gap for $CaTiO_3$ with much more perfect crystal structure and higher phase purity after treatment by 2% NaOH solution is 3.50 eV while that for the untreated $CaTiO_3$ is 3.10 eV [19]. They thought that the 0.4 eV narrower band gap for the untreated $CaTiO_3$ can be ascribed to the energy level of defects within the forbidden band, and this lower crystal perfection also resulted in the tail (with higher absorbance) in the visible light region of the DRS spectrum for the untreated $CaTiO_3$. Moreover, Pontes and co-workers have proved that the visible PL emission in amorphous $CaTiO_3$ was directly related to the exponential optical edges and tails [20]. The nature of these exponential optical edges and tails may be associated with defects promoted by the disordered structure of the amorphous materials [20]. Furthermore, the large amount of "broken" surfaces or dangling bonds and defect centers intrinsically existing in the hydrothermal samples due to the very thin flaky morphologies and the smaller crystallite size, can also form various animated energy levels localized within the forbidden gap and they act as optical absorption centers, which make large modifications in the optical properties of the materials, and are responsible for the more visible absorbance than the SSR sample [20]. Therefore, the nature of red-shift of UV absorption and tails for the hydrothermal samples compared with the SSR sample can be mainly attributed to the specific morphologies and/or the lower crystal perfections as described above.

Photoactivities of the $La_2Ti_2O_7$ prepared by the hydrothermal and SSR method for water splitting were also measured under UV irradiation. Table 1 summarizes the results of water photosplitting and the surface areas of the obtained samples. As shown in table 1, the photoactivity of the obtained samples increased as the hydrothermal temperature increased from 210 to 240 °C, although sample derived from 210 °C has a higher surface area (82 m^2/g) than that (54 m^2/g) of sample derived from 240 °C. This might be ascribed to the presence of little noncrystallized phase in the low temperature sample. However, although the SSR sample has much higher and more perfect crystallinity compared with the hydrothermal samples, it showed no significant photoactivity. Therefore, in addition to the surface area and crystallinity, other factors governing the photoactivity in water splitting should be considered to explain the variation among those samples.

The hydrothermal synthesis provides mixing of elements at an atomic level, which can reduce the diffusion path needed for obtaining the desired material down to the nanometer scale, and thus, needs a lower temperature to obtain the crystal phase than the SSR method. Therefore, compared with the SSR method, the effects of hydrothermal process on $La_2Ti_2O_7$ could be summarized as follows: higher surface areas, higher phase purity, smaller crystallite size, lower agglomeration and crystal perfections. Consequently, all these desirable properties led to a higher photoactivity. In addition to the much lower surface area compared with samples derived from hydrothermal processes, SSR sample has higher bandgap energy as shown in the DRS of figure 5, which result in the smaller amount of light absorption in the longer wave region of Hg lamp. Thus, the low photocatalytic activity of SSR sample appears to be closely related to the effect of lower surface areas and higher bandgap energy. Furthermore, the smaller crystallite sizes for the hydrothermal samples are also an important factor for improving the photoactivity, which is beneficial for the separation and diffusion of the photogenerated carriers due to the

much shorter diffusion path than the SSR sample. The thin planar morphologies also favor the interaction between the photogenerated carriers and water molecules on the surface of photocatalysts, and the light penetration in the suspension system, those factors together with the red-shift of UV absorption for hydrothermal samples can lead to the more efficient light absorption of photocatalyst. Therefore, relative to the SSR sample, the flaky $La_2Ti_2O_7$ showed higher surface areas, lower bandgap energy, and shorter diffusion distances of carriers due to the smaller crystallite size, lower agglomeration and crystal perfections. All these factors led to the higher photoactivity for the hydrothermal samples during the water photosplitting.

In summary, flaky $La_2Ti_2O_7$ with monoclinic structures have been prepared through a hydrothermal process by using CTAB as surfactant and NaOH as mineralizer. The results of XRD, SEM and TEM indicated that $La_2Ti_2O_7$ crystals were formed under hydrothermal treatment at 210–240 °C for 20–24 h. Compared with SSR methods, the present method is a mild, effective process for the preparation of $La_2Ti_2O_7$. Among various obtained $La_2Ti_2O_7$, only samples derived from hydrothermal process produced H_2 from photocatalytical water splitting under UV irradiation, while there is no significant H_2 production detected over the SSR sample. Photocatalytic activity of the flaky $La_2Ti_2O_7$ derived from the hydrothermal process depended on its higher surface areas and phase purity, much smaller crystal size, more efficient light absorption and charge separation due to its special thin planar morphologies and smaller crystallite size.

Acknowledgments

This work was supported by Natural Science Foundation (20573078) of China, National "863" Foundation (2006AA03Z344), Talented Young Scientist Foundation (2006ABB003) of Hubei Province and the Natural Science Fund (2004ABA083) of Hubei Province, China.

References

[1] D.W. Hwang, H.G. Kim, J.S. Lee, J. Kim and W. Li, J. Phys. Chem. 109 (2005) 2093.
[2] D.W. Hwang, K.Y. Cha, J. Kim, H.G. Kim, G. Hyun, S.W. Bae and J.S. Lee, Ind. Eng. Chem. Res. 42 (2003) 1184.
[3] H.G. Kim, D.H. Hwang, S.W. Bae, J.H. Jung and J.S. Lee, Catal. Lett. 91 (2003) 193.
[4] M. Suresh, A.V. Prasadarao and S. Komarneni, J. Electroceram. 6 (2001) 147.
[5] Z.T. Zhao, Y.M. Zhang, J. Yang, H. Li, W. Song and X.Q. Zhao, J. Ceram. Soc. Jpn. 113 (2005) 67.
[6] P.A. Fuierer and E. Newnham, J. Am. Ceram. Soc. 74 (1991) 2876.
[7] D.W. Hwang, J.S. Lee, W. Li and S.H. Oh, J. Phys. Chem. 107 (2003) 4963.
[8] A.V. Prasadarao, U. Selvaraj, S. Komarneni and A.S. Bhalta, Mater. Lett. 12 (1991) 306.
[9] D.S. Todorovsky, M.M. Getsova and M.A. Vasileva, J. Mater. Sci. 37 (2002) 4029.
[10] M. Kakihana and M. Yoshimura, Bull. Chem. Soc. Jpn. 72 (1999) 1427.
[11] M.M. Milanova, M. Kakihana, M. Arima, M. Yashima and M. Yoshimura, J. Alloys Compd. 242 (1996) 6.
[12] S. Ikeda, M. Hara, J.N. Kondo and K. Domen, Chem. Mater. 10 (1998) 72.
[13] H.G. Kim, D.W. Hwang, J. Kim, Y. Kim and J.S. Lee, Chem. Commun. 999 (1999) 1077.
[14] D.W. Hwang, H.G. Kim, J. Kim, Y.G. Kim and J.S. Lee, J. Catal. 103 (2000) 40.
[15] J. Kim, D.W. Hwang, H.G. Kim, S.W. Bae, Y.G. Kim, S.M. Ji and J.S. Lee, Chem. Commun. 2 (2002) 2488.
[16] D. Chen and R. Xu, Mater. Res. Bull. 33 (1998) 409.
[17] E.B. Panasenk and R.G. Begunova, J. Inorg. Chem. 29 (1984) 1430.
[18] T. Ohno, T. Tsubota, M. Toyofuku and R. Inaba, Catal. Lett. 98 (2004) 255.
[19] G.B. Wang, Y.J. Wang, X.Q. Zhao and H.T. Zhang, Chin. J. Catal. 26 (2005) 138.
[20] F.M. Pontes, C.D. Pinheiro, E. Longo, E.R. Leite, S.R. de Lazaro, J.A. Varela, P.S. Pizani, T.M. Boschi and F. Lanciotti, Mater. Chem. Phys. 78 (2002) 227.